Hybrid (bolted/bonded)joints applied to aeronautic parts: analytical two-dimensional model of a single-lap joint

Eric Paroissien, Marc Sartor, Jacques Huet, Frederic Lachaud

Hybrid (Bolted/Bonded) Joints Applied to Aeronautic Parts: Analytical Two-Dimensional Model of a Single-Lap Joint

Eric Paroissien[*], Marc Sartor[†], Jacques Huet[‡], and Frédéric Lachaud[§]
Institut de Génie Mécanique, Toulouse, 31062, FRANCE

The mechanical behavior of hybrid (bolted/bonded) joints is investigated. The joints under study are balanced single-lap joints, and an elastic behavior of the materials is assumed. A fully parametric analytical two-dimensional model, based on the Finite Element Method, is presented. A special Finite Element ("*Bonded Beams*" element) is computed in order to simulate the bonded adherends. The simulation of fasteners is examined through experimental and numerical approaches. Good agreement was found between the experimental and numerical results.

Nomenclature

C_u	=	stiffness (N.mm^{-1}) of the spring in the x direction (longitudinal stiffness)
C_w	=	stiffness (N.mm^{-1}) of the spring in the y direction (transversal stiffness)
C_θ	=	stiffness (N.mm.rad^{-1}) of the spring around the z direction (bending stiffness)
E_f	=	Young's modulus (MPa) of the fastener
E_{pt}	=	total potential energy (N.mm)
E_r	=	Young's modulus (MPa) of the adherends
E_s	=	Young's modulus (MPa) of in the adhesive
F	=	force vector
G_s	=	Coulomb's modulus (MPa) of the adhesive
I_r	=	second moment of area (mm^4) of the adherends ($12I_r=e_r^3 b$)
$K,\ \widetilde{K}$	=	stiffness matrix
K_{BB}	=	stiffness matrix of the "*Bonded Beams*" element
L	=	length (mm) of the overlap
M_a	=	moment (N.mm) in the adherend α around the z direction
N_α	=	force (N) in the adherend α in the x direction
Q_β	=	nodal force (N) applied to the node β in the x direction
R	=	reducing matrix
R_β	=	nodal force (N) applied to the node β in the y direction
S	=	adhesive peel stress (MPa)
S_r	=	section (mm^2) of the adherends ($S_r=e_r b$)
S_β	=	nodal moment (N.mm) applied to the node β around the z direction
T	=	adhesive shear stress (MPa)
V_α	=	force (N) in the adherend α in the y direction
b	=	width (mm) of the adherends (lateral pitch between two rows of fasteners)
d	=	length (mm) between the end of the joint and the nearest fastener
e_r	=	thickness (mm) of the adherends

[*] Ph.D. Student, Département de Génie Mécanique, Ecole Nationale Supérieure d'Ingénieurs de Constructions Aéronautiques, eric.paroissien@ensica.fr.
[†] Professor, Département de Génie Mécanique, Institut National des Sciences Appliquées de Toulouse, marc.sartor@insa-toulouse.fr.
[‡] Professor, Département de Génie Mécanique, Ecole Nationale Supérieure d'Ingénieurs de Constructions Aéronautiques, jacques.huet@ensica.fr.
[§] Assistant Professor, Département de Génie Mécanique, Ecole Nationale Supérieure d'Ingénieurs de Constructions Aéronautiques, frederic.lachaud@ensica.fr.

e_s = thickness (mm) of the adhesive
f = force (N) applied to the joint in the x direction
h = generic function
l = length (mm) of the beams outside the overlap
m = generic index
n = number of fasteners
$q,\ \tilde{q}$ = displacements vector
s = length (mm) of the longitudinal pitch between two lines of fasteners
u = displacement (mm) in the x direction
w = displacement (mm) in the y direction
Δ = length (mm) of a "*Bonded Beams*" element
ϕ = diameter (mm) of the fastener
α = generic subscript which refers to the adherend α
β = generic subscript which refers to the node β
ν_r = Poisson's ratio of the adherend
ν_s = Poisson's ratio of the adhesive
ν_f = Poisson's ratio of the fastener
θ = angular displacement (rad) around the z direction
(x,y,z) = direct orthonormal base

I. Introduction

THIS paper deals with the load transfer in hybrid (bolted/bonded) single-lap joints. The joints of civil aircraft are investigated. The first investigation case is the longitudinal joint, typical in fuselage structures. These joints are composed of aluminum sheets and titanium bolts. The developed method, which is presented in this paper, can also be applied to other joints on aircraft.

Hybrid joints are bolted/bonded joints, then associating a discrete transfer mode with a continuous one, each one belonging to its own stiffness. The bolted joint (discrete transfer mode) generates a high stress around the fastener holes which is detrimental to the fatigue resistance. The bonded joint (continuous transfer mode) allows a better distribution of the load; however the adhesive presents a viscoplastic behavior depending on the environmental conditions which is prejudicial to the static strength in the long term. With regard to aircraft structure assembly, hybrid joining could be interesting because it could reduce the load transferred by the fasteners in order to improve the fatigue life, while ensuring static strength under extreme loads. The idea is to design the hybrid joint in order to share the load between the adhesive and the fasteners in a suitable way. That's why the influence of the joint geometry and the material properties on the load transfer are investigated by means of developing efficient designing tools. Analytical approaches are thus preferred.

One-dimensional methods for the calculation of bolted joints and numerous two-dimensional methods for the calculation of bonded joints exist. In this paper a parametric analytical approach for the calculation of hybrid joints involving bonded and bolted methods is presented. Thanks to the analytical model a campaign of tests is launched in

order to validate the analytical model and as well as a parametric three-dimensional numerical model within this study. The numerical model has in particular the ability to improve the model of fasteners in the analytical model. This cross validation aims at defining the efficiency domain of each model. Consequently, three approaches are presented: an analytical analysis, experimental tests and numerical analyses.

II. Analytical Model for Bolted Joints

The load transfer in a bolted joint is a discrete transfer mode. It means that between each bolt, or on each bay, the transferred load is constant.

The fatigue life of a bolted joint can be determined from the bolt load transfer. The load transferred by the fasteners can be obtained analytically by recurrence[1] or by using an analogy with an electric meshing.[2,3] The fasteners are usually simulated by springs, which are considered to work by shearing. The main parameter is the rigidity of these shearing springs.

The behavior of a fastener in a joint is a complex problem and the determination of its flexibility has been the subject of numerous studies and formulations.[1,4-8] The behavior of a fastener can be defined by a force-displacement curve of the joint. The linear part of this curve provides the rigidity of the fastener (Fig. 1), quoted *C*. This value corresponds to the integral displacement, which is composed of the deformations due to shear, bending and bearing loads, of the fastener in the bolted joint.

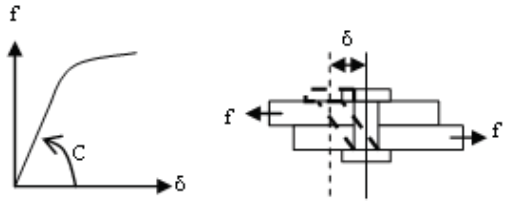

Fig. 1 Behavior of a fastener in a single-lap joint subject to in-plane shear loading.

III. Analytical Model for Bonded Joints

Numerous publications exist investigating the behavior of bonded joints. The single-lap joint was firstly investigated by Volkersen[9] in 1938 and it led to the distribution of the adhesive shear stress integrating the local equilibrium equations of the adherends and simulating the adhesive by an infinite number of shearing elastic springs. However, the large displacements of the joint due to the eccentricity of the load path have not been considered in this previous study. In 1944, Goland and Reissner[10] (G&R) took into account the effect of this eccentricity of load

path and determined the adhesive peel and shear stresses. The adhesive was simulated by an infinite number of tensile and shearing elastic springs, but the thickness of the adhesive was considered negligible. In the 70's Hart-Smith[11,12] provided a voluminous work on bonded joints considering the single and double-lap joint configuration, the balanced and unbalanced configuration, the elastic and elastic-plastic behavior of the adhesive. Moreover, Hart-Smith considered the geometrical effect of the thickness of the adhesive on the stress and load functions in the joint. The adhesive was simulated in the same way as the previous one. However, this simulation of the adhesive does not allow verification of the adhesive free stress state at the end of the joint. Other authors[13,14] provide analytical formulations which show the adhesive free stress state at the end of the joint: the maximum of adhesive shear or peel stresses is no longer at the end of the joint but is displaced in the lap joint and higher.

In this paper the approach of the bonded joint corresponds to the approach of G&R,[10] since this work aims at developing an easy to use and robust tool for analyzing the mechanical behavior of the hybrid joints. Hence the local equilibrium equations which are considered are (Eq. (1)):

$$\begin{cases} \dfrac{1}{b}\dfrac{dN_1}{dx} + T = 0 \\ \dfrac{1}{b}\dfrac{dN_2}{dx} - T = 0 \\ \dfrac{1}{b}\dfrac{dV_1}{dx} - S = 0 \\ \dfrac{1}{b}\dfrac{dV_2}{dx} + S = 0 \\ \dfrac{dM_1}{dx} + V_1 + 0.5be_r T = 0 \\ \dfrac{dM_2}{dx} + V_2 + 0.5be_r T = 0 \end{cases} \tag{1}$$

The relations between displacements and loads are given by Eq. (2) for the generic index α equal to *1* and *2*:

$$\begin{cases} \dfrac{du_\alpha}{dx} = \dfrac{N_\alpha}{E_\alpha S_\alpha} \\ \dfrac{d^2 w_\alpha}{dx^2} = \dfrac{M_\alpha}{E_\alpha I_\alpha}, \alpha = 1,2 \\ \theta_\alpha = \dfrac{dw_\alpha}{dx} \end{cases} \tag{2}$$

Finally the adhesive is considered elastic and is simulated by an infinite number of tensile springs:

$$T = \frac{G_s}{e_s}\left(u_2 - u_1 - \frac{1}{2}e_r(\theta_1 + \theta_2)\right) \tag{3}$$

$$S = \frac{E_s}{e_s}(w_1 - w_2) \tag{4}$$

The relations given in Eq. (1) to (4) are the basic equations used in the analytical approach of hybrid joints, which is presented here.

IV. Two-Dimensional Analytical Model for Hybrid (Bolted/Bonded) Joints

The analytical approach based on discontinuous method is used for stepped-joints.[15] The idea of developing designing tools thanks to a microcomputer program is widespread.[16-18] The Finite Element Method (FEM) is well adapted to this idea.

The FEM is used for developing the two-dimensional analytical model of a hybrid balanced single-lap joint. The presented approach in this paper can be applied in the one-dimensional case and provide the same results as the method based on the direct integration of the local equilibrium equations.[19] Moreover the use of the FEM is flexible since different boundaries conditions can be applied easily. That's why the FEM approach is chosen for this two-dimensional derivation. The hypotheses are: a constant thickness of the adhesive along the overlap, an elastic behavior of the adhesive and of the adherends. Moreover, the geometrical and mechanical parameters and the number, quoted *n*, of fasteners are free. However, the presented joint is a balanced joint in order to simplify the mathematical derivation of the model.

A two-dimensional approach is required in order to consider the effects of the bending of the adherends, due to the eccentricity of the load path, and the effects on the adhesive peel stress. Hence, the single-lap joint is meshed in two-dimensional elements as shown in Fig. 2. The parts outside the overlap are simulated by beam elements which have two nodes and three degrees of freedom per node. The fasteners are simulated by rigid bodies of which both nodes are connected with the other nodes of the structure by two translational springs and one rotational spring. The *n* fasteners are splitting the lap joint in *(n+1)* parts representing the bonded bays. Each bonded part is simulated by a new element called "*Bonded Beams*" (BB), which have four nodes and three degrees of freedom (DoF) per node. Consequently, the BB element represents the adherends and the adhesive at the same time. The four nodes of this

element allow to take into account the relative displacements of the adherends and only one BB element is required for each bonded bay of the lap. The stiffness matrix of the BB element has to be determined.

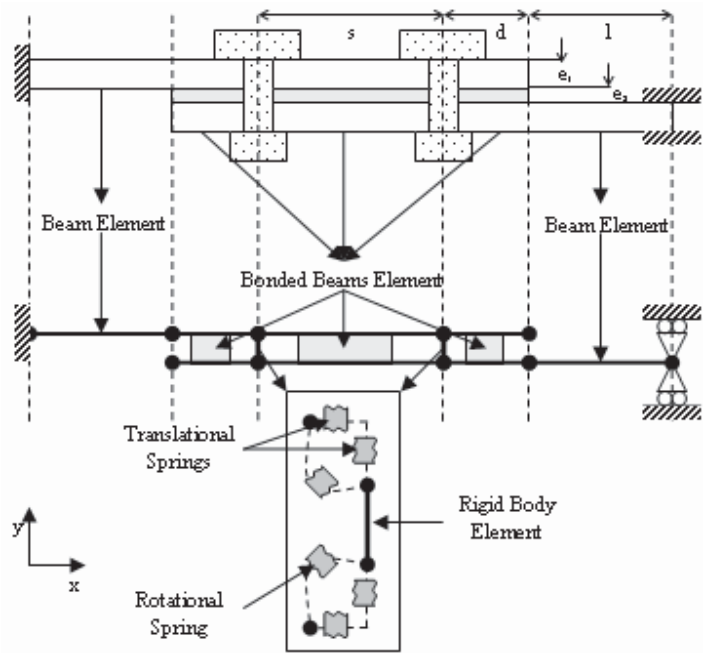

Fig. 2 Meshing of the hybrid single-lap joint with two-dimensional elements.

A. Stiffness matrix of the "*Bonded Beams*" element

The first step is to determine the displacements in each adherend for the bonded joint configuration. The picture given in Fig. 3 represents the considered displacements in a BB element. The four nodes are quoted *i*, *j*, *k, l* and the length of the BB element is quoted Δ.

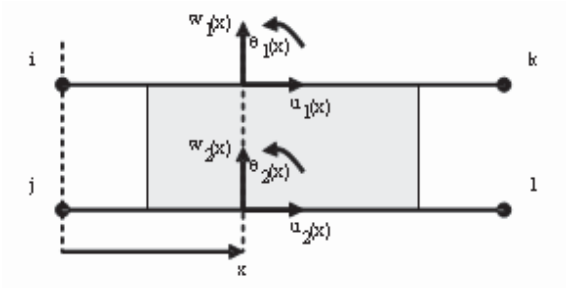

Fig. 3 Displacements in the "*Bonded Beams*" element.

The Eq. (1) to (4) allow to determine the linear system of differential equations. This system can be solved using the linear relations given in Eq. (5) for the generic function *h*:

$$\begin{cases} S_h = h_2 + h_1 \\ D_h = h_2 - h_1 \end{cases} \tag{5}$$

The linear system of differential equations which are obtained is given in Eq. (6):

$$\begin{cases} \dfrac{d^2 D_u}{dx^2} - \eta^2 D_u = -\dfrac{e_r}{2}\eta^2 \dfrac{dS_w}{dx} \\ \dfrac{d^2 S_u}{dx^2} = 0 \\ \dfrac{d^4 D_w}{dx^4} + 4\sigma^4 D_w = 0 \\ \dfrac{d^4 S_w}{dx^4} - \mu^2 \dfrac{d^2 S_w}{dx^2} = -\dfrac{2}{e_r}\mu^2 \dfrac{dD_u}{dx} \end{cases} \tag{6}$$

where the constants η, μ and σ are given by the Eq. (7) to (9):

$$\eta^2 = \frac{2G_s}{e_s e_r E_r} \tag{7}$$

$$\mu^2 = \frac{b e_r^2 G_s}{2 e_s E_r I_r} \tag{8}$$

$$\sigma^4 = \frac{b E_s}{2 e_s E_r I_r} \tag{9}$$

The solution of the linear system, using the following quoting given in Eq. (10), is:

$$\begin{cases} \cosh(z)\cos(z) = chc(z) \\ \sinh(z)\sin(z) = shs(z) \\ \sinh(z)\cos(z) = shc(z) \\ \cosh(z)\sin(z) = chs(z) \end{cases} \tag{10}$$

$$S_u = c_1 x + c_2 \tag{11}$$

$$D_w = c_3 chc(\sigma x) + c_4 shs(\sigma x) + c_5 chs(\sigma x) + c_6 shc(\sigma x) \tag{12}$$

$$D_u = c_7 e^{-\rho x} + c_8 e^{\rho x} + c_9 + c_{10} x + c_{11} x^2 \tag{13}$$

$$S_w = c_{12} + \left(c_9 - 2\eta^{-2}c_{11}\right)\frac{2}{e_r}x + \frac{2}{e_r}c_{10}\frac{x^2}{2} + \frac{2}{e_r}c_{11}\frac{x^3}{3} + \frac{2}{e_r}\frac{\mu^2}{\eta^2}\frac{1}{\rho}\left(c_7 e^{-\rho x} - c_8 e^{\rho x}\right) \tag{14}$$

where c_1 to c_{12} are the integration constants (given in Appendix), and:

$$\rho^2 = \eta^2 + \mu^2 \tag{15}$$

The functions D_θ and S_θ are obtained by differentiation from Eq. (12) and (4) respectively. The 12 integration constants are found with the 12 boundaries conditions, corresponding to the 12 DoF of the BB element; the integration constants are thus functions of the 12 DoF. The displacements are obtained by inversing the linear relations given in Eq. (5).

$$u_1 = \frac{1}{2}\left[\left(c_2 - c_9\right) + \left(c_1 - c_{10}\right)x - c_{11}x^2 - c_7 e^{-\rho x} - c_8 e^{\rho x}\right] \tag{16}$$

$$u_2 = \frac{1}{2}\left[\left(c_2 + c_9\right) + \left(c_1 + c_{10}\right)x + c_{11}x^2 + c_7 e^{-\rho x} + c_8 e^{\rho x}\right] \tag{17}$$

$$w_1 = \frac{1}{2}\begin{bmatrix} c_{12} + \left(c_9 - 2c_{11}\eta^{-2}\right)\frac{2}{e_r}x + \frac{2}{e_r}c_{10}\frac{x^2}{2} + \frac{2}{e_r}c_{11}\frac{x^3}{3} + \frac{2}{e_r}\frac{\mu^2}{\eta^2}\frac{1}{\rho}\left(c_7 e^{-\rho x} - c_8 e^{\rho x}\right) \\ - c_3 chc(\sigma x) - c_4 shs(\sigma x) - c_5 chs(\sigma x) - c_6 shc(\sigma x) \end{bmatrix} \tag{18}$$

$$w_2 = \frac{1}{2}\begin{bmatrix} c_{12} + \left(c_9 - 2c_{11}\eta^{-2}\right)\frac{2}{e_r}x + \frac{2}{e_r}c_{10}\frac{x^2}{2} + \frac{2}{e_r}c_{11}\frac{x^3}{3} + \frac{2}{e_r}\frac{\mu^2}{\eta^2}\frac{1}{\rho}\left(c_7 e^{-\rho x} - c_8 e^{\rho x}\right) \\ + c_3 chc(\sigma x) + c_4 shs(\sigma x) + c_5 chs(\sigma x) + c_6 shc(\sigma x) \end{bmatrix} \tag{19}$$

$$\theta_1 = \frac{1}{2}\begin{bmatrix} \left(c_9 - 2c_{11}\eta^{-2}\right)\frac{2}{e_r} + \frac{2}{e_r}\alpha_{10}x + \frac{2}{e_r}\alpha_{11}x^2 - \frac{2}{e_r}\frac{\mu^2}{\eta^2}\left(c_7 e^{-\rho x} + c_8 e^{\rho x}\right) \\ - c_3\sigma\left(shc(\sigma x) - chs(\sigma x)\right) - c_4\sigma\left(chs(\sigma x) + shc(\sigma x)\right) - c_5\sigma\left(shs(\sigma x) + chc(\sigma x)\right) - c_6\sigma\left(chc(\sigma x) - shs(\sigma x)\right) \end{bmatrix} \tag{20}$$

$$\theta_2 = \frac{1}{2}\begin{bmatrix} \left(c_9 - 2c_{11}\eta^{-2}\right)\frac{2}{e_r} + \frac{2}{e_r}c_{10}x + \frac{2}{e_r}\alpha_{11}x^2 - \frac{2}{e_r}\frac{\mu^2}{\eta^2}\left(c_7 e^{-\rho x} + c_8 e^{\rho x}\right) \\ + c_3\sigma\left(shc(\sigma x) - chs(\sigma x)\right) + c_4\sigma\left(chs(\sigma x) + shc(\sigma x)\right) + c_5\sigma\left(shs(\sigma x) + chc(\sigma x)\right) + c_6\sigma\left(chc(\sigma x) - shs(\sigma x)\right) \end{bmatrix} \tag{21}$$

From the previous expressions of displacements (Eq. (16) to (21)) and from the relations given in Eq. (2) the forces in the adherends are given by:

$$N_1 = \frac{E_r S_r}{2}\left[(c_1 - c_{10}) - 2c_{11}x - \rho\left(c_7 e^{\rho x} - c_8 e^{-\rho x}\right)\right] \tag{22}$$

$$N_2 = \frac{E_r S_r}{2}\left[(c_1 + c_{10}) + 2c_{11}x + \rho\left(c_7 e^{\rho x} - c_8 e^{-\rho x}\right)\right] \tag{23}$$

$$M_1 = \frac{E_r I_r}{2}\left[\frac{2}{e_r}c_{10} + \frac{2}{e_r}2c_{11}x - \frac{2}{e_r}\frac{\mu^2}{\eta^2}\rho\left(c_7 e^{\rho x} - c_8 e^{-\rho x}\right) - 2\sigma^2\left(-c_3 shs(\sigma x) + c_4 chc(\sigma x) + c_5 shc(\sigma x) - c_6 chs(\sigma x)\right)\right] \tag{24}$$

$$M_2 = \frac{E_r I_r}{2}\left[\frac{2}{e_r}c_{10} + \frac{2}{e_r}2c_{11}x - \frac{2}{e_r}\frac{\mu^2}{\eta^2}\rho\left(c_7 e^{\rho x} - c_8 e^{-\rho x}\right) + 2\sigma^2\left(-c_3 shs(\sigma x) + c_4 chc(\sigma x) + c_5 shc(\sigma x) - c_6 chs(\sigma x)\right)\right] \tag{25}$$

$$V_1 = -\frac{E_r I_r}{2}\left[\frac{2}{e_r}2c_{11} - \frac{2}{e_r}\frac{\mu^2}{\eta^2}\rho^2\left(c_7 e^{\rho x} + c_8 e^{-\rho x}\right) - 2\sigma^3\begin{pmatrix}-c_3\left(chs(\sigma x) + shc(\sigma x)\right) + c_4\left(shc(\sigma x) - chs(\sigma x)\right)\\ + c_5\left(chc(\sigma x) - shs(\sigma x)\right) - c_6\left(chc(\sigma x) + shs(\sigma x)\right)\end{pmatrix}\right] - \frac{1}{2}e_r bT \tag{26}$$

$$V_2 = -\frac{E_r I_r}{2}\left[\frac{2}{e_r}2c_{11} - \frac{2}{e_r}\frac{\mu^2}{\eta^2}\rho^2\left(c_7 e^{\rho x} + c_8 e^{-\rho x}\right) + 2\sigma^3\begin{pmatrix}-c_3\left(chs(\sigma x) + shc(\sigma x)\right) + c_4\left(shc(\sigma x) - chs(\sigma x)\right)\\ + c_5\left(chc(\sigma x) - shs(\sigma x)\right) - c_6\left(chc(\sigma x) + shs(\sigma x)\right)\end{pmatrix}\right] - \frac{1}{2}e_r bT \tag{27}$$

From the Eq. (22) to (27), the nodal forces (Fig. 4) can be deduced using the following relations:

$$\begin{cases} Q_i = -N_1(0) \\ Q_j = -N_2(0) \\ Q_k = N_1(\Delta) \\ Q_l = N_2(\Delta) \end{cases} \tag{28}$$

$$\begin{cases} R_i = -V_1(0) \\ R_j = -V_2(0) \\ R_k = V_1(\Delta) \\ R_l = V_2(\Delta) \end{cases} \tag{29}$$

$$\begin{cases} S_i = -M_1(0) \\ S_j = -M_2(0) \\ S_k = M_1(\Delta) \\ S_l = M_2(\Delta) \end{cases} \tag{30}$$

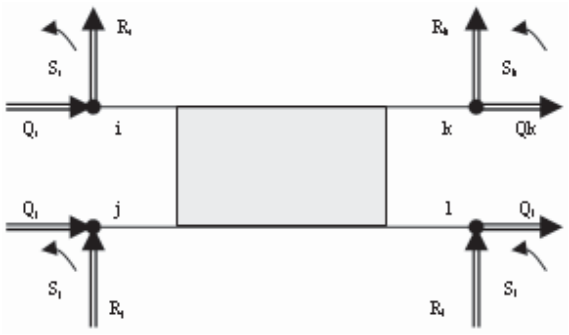

Fig. 4 Nodal forces in the "*Bonded Beams*" element

Finally, the stiffness matrix of the BB element, which is quoted K_{BB}, and the size of which is *[12;12]*, is computed from the nodal forces and the nodal displacements:

$$K_{BB} = \begin{pmatrix} \left[\frac{\partial Q_\sigma}{\partial u_\tau}\right] & \left[\frac{\partial Q_\sigma}{\partial w_\tau}\right] & \left[\frac{\partial Q_\sigma}{\partial \theta_\tau}\right] \\ \left[\frac{\partial R_\sigma}{\partial u_\tau}\right] & \left[\frac{\partial R_\sigma}{\partial w_\tau}\right] & \left[\frac{\partial R_\sigma}{\partial \theta_\tau}\right] \\ \left[\frac{\partial S_\sigma}{\partial u_\tau}\right] & \left[\frac{\partial S_\sigma}{\partial w_\tau}\right] & \left[\frac{\partial S_\sigma}{\partial \theta_\tau}\right] \end{pmatrix}, \sigma, \tau = i, j, k, l \tag{31}$$

B. Stiffness matrix of the structure

The conventional stiffness matrix of a beam (Appendix) corresponding to the beams outside the overlap is taken.

For n fasteners, the structure is composed of $2n+6$ nodes: that is corresponded to $6n+18$ DoF. A rigid body element is associated to each fastener. This rigid body is coupled with three springs, the stiffnesses of which being quoted $2C_u$, $2C_w$ and $2C_\theta$. The fastener m is placed between the nodes $2(m+1)$ and $2(m+1)+1$ of the structure. Both nodes of the rigid body element are quoted $r(m)$ and $s(m)$ as shown in the Fig. 5. Hence, the structure is composed of $4n+6$ nodes and $12n+18$ DoF.

The partial stiffness matrix of the fastener m, quoted K_u^m and written in the base $(u_{2m+2} ; u_{2m+3} ; u_{r(m)} ; u_{s(m)})$ considering the displacements according to x only, is also given by:

$$K_u^m = 2\begin{pmatrix} C_u & 0 & -C_u & 0 \\ 0 & C_u & 0 & -C_u \\ -C_u & 0 & C_u & 0 \\ 0 & -C_u & 0 & C_u \end{pmatrix}, m \in [1; n] \tag{32}$$

The same relations are obtained for the partial rigidity K_w^m and K_θ^m. Consequently, the introduction of the *n* rigid bodies induces the following *3n* equilibrium relations and *3n* associated relations of kinematic linear dependence:

$$\begin{cases} -Q_{s(m)} - Q_{r(m)} = 0 \\ -R_{s(m)} - R_{r(m)} = 0 \\ -S_{s(m)} - S_{r(m)} - e_r Q_{r(m)} = 0 \end{cases} \quad ,m \in [1;n] \tag{33}$$

$$\begin{cases} u_{s(m)} = u_{r(m)} + e_r \theta_{r(m)} \\ w_{s(m)} = w_{r(m)} \\ \theta_{r(m)} = \theta_{s(m)} \end{cases} \quad ,m \in [1;n] \tag{34}$$

Consequently, the size of the displacements vector is decreasing from *12n+18* to *9n+18*, and the range of the stiffness matrix of the structure is also decreasing by *3n*. The problem is treated by the Master-Slave method.[20] It is chosen to eliminate the DoF $u_{s(m)}$, $w_{s(m)}$ and $\theta_{s(m)}$. Utilising Eq. (34) a reduction matrix *R*, the size of which is *[12n+18;9n+18]*, can be defined:

$$q = R\tilde{q} \tag{35}$$

Hence, it comes:

$$E_{pt} = \frac{1}{2} q^t K q - q^t F = \frac{1}{2} \tilde{q}^t R^t K R \tilde{q} - \tilde{q}^t R^t F \tag{36}$$

And finally, the expression of the total potential energy becomes:

$$E_{pt} = \frac{1}{2} \tilde{q}^t \tilde{K} \tilde{q} - \tilde{q}^t \tilde{F} \tag{37}$$

where:

$$\begin{cases} \tilde{K} = R^t K R \\ \tilde{F} = R^t F \end{cases} \tag{38}$$

The displacements vector, which is minimizing Eq. (38), verifies:

$$\widetilde{K}\widetilde{q} = \widetilde{F} \tag{39}$$

A microcomputer program is also developed using the MATLAB[21] mathematical code, in order to calculate the solution of the Eq. (39).

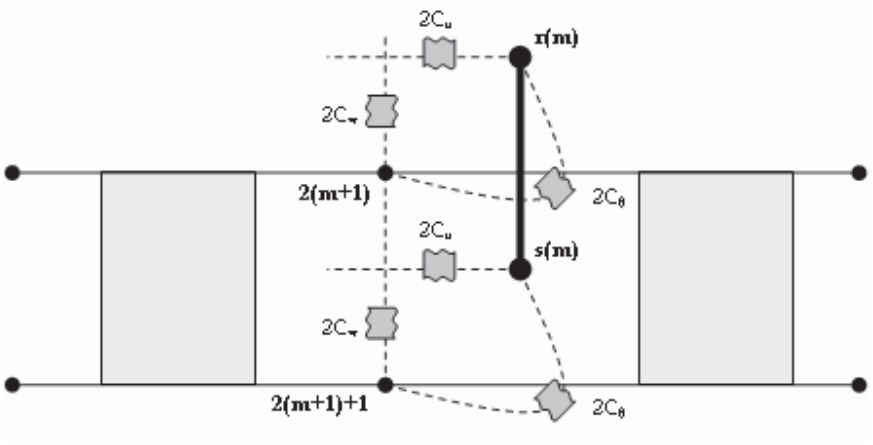

Fig. 5 A rigid body with the springs between the nodes 2(m+1) and 2(m+1)+1 simulating the fastener m.

C. Results for the Bonded and the Bolted Single-Lap Joint Configurations: both Boundaries Cases

In order to check the ability of the BB element to simulate the bonded joint, the model is tested without any fastener, and compared with the results given by the G&R[10] analysis. The mechanical and geometrical parameters of the joint under consideration are given in Table 1. For this configuration, the moment factor[10], which is calculated thanks to the G&R[10] model, is equal to 0.875. Consequently, for the comparison, we choose the length of the beam outside the overlap, which provides the same moment factor. The adhesive shear stress and the peel stress are plotted in Fig. 6 and Fig. 7 respectively. It can be noticed that the curves are superposed. The simulation of a single-lap bonded joint using the BB element shows hence a good agreement with the G&R[10] theory. Consequently, it is reasonable to think that the BB element can be used in order simulate the bonded parts of the hybrid single-lap joint.

Table 1 Mechanical and geometrical parameters

E_r, MPa	ν_r	e_r, mm	G_s, MPa	ν_s	e_s, mm	b, mm	L,mm	d, mm
72000	0.3	2.4	200	0.35	0.6	19.2	38.4	9.6

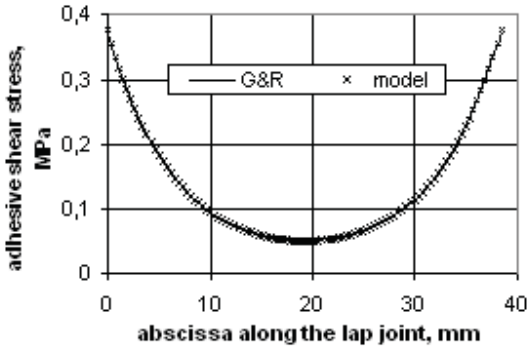

Fig. 6 Adhesive shear stress along the lap joint, G&R vs. model with f = 100 N.

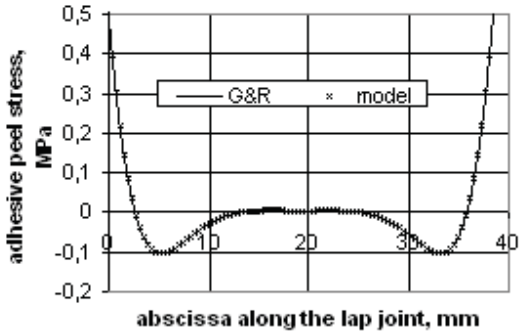

Fig. 7 Adhesive peel stress along the lap joint, G&R vs. model with f = 100 N.

To check the ability of the model to simulate the bolted joints, the same configuration as the previous one is chosen except for the adhesive parameters: the Coulomb's modulus of the adhesive (i.e.: G_s) has to be as low as possible (for example 1.10^{-3} MPa.mm^{-1}). No analytical model dedicated to the bolted joints and similar to the one presented was found in the literature. Also, in order to check the results given by the proposed model, a Finite Element (FE) model is developed using the commercial code IDEAS.[22] This FE model is composed of beam elements, rigid bodies, translational and rotational springs, and boundaries conditions, so that it is equivalent to the proposed model in the bolted configuration. The complementary data used to design this model are: s = 19.2 mm (longitudinal pitch between two lines of fasteners), e_s = 0 mm and l = 70 mm (length of the beams outside the overlap). In addition, the stiffnesses of the springs are taken as follow: 5.10^4 N.mm^{-1} for the longitudinal stiffness (i.e.: C_u), 2.10^6 N.mm^{-1} for the transversal stiffness (i.e.: C_w) and 6.10^6 N.mm.rad^{-1} for the bending stiffness (i.e.: C_θ). These values could be chosen arbitrary for the demonstration; however, they are taken close to the values from the 3D numerical analysis, presented in paragraph VI. Three configurations of the joint are analyzed successively,

considering the use of one, two and three fasteners, as shown in Fig. 8. Some characteristic results obtained from this FE model are given in the Table 2. The microcomputer program developed with the MATLAB[21] code for the analytical approach proposed in this paper leads to the same results. Consequently, the analytical model seems to be able to simulate the bolted joint configuration.

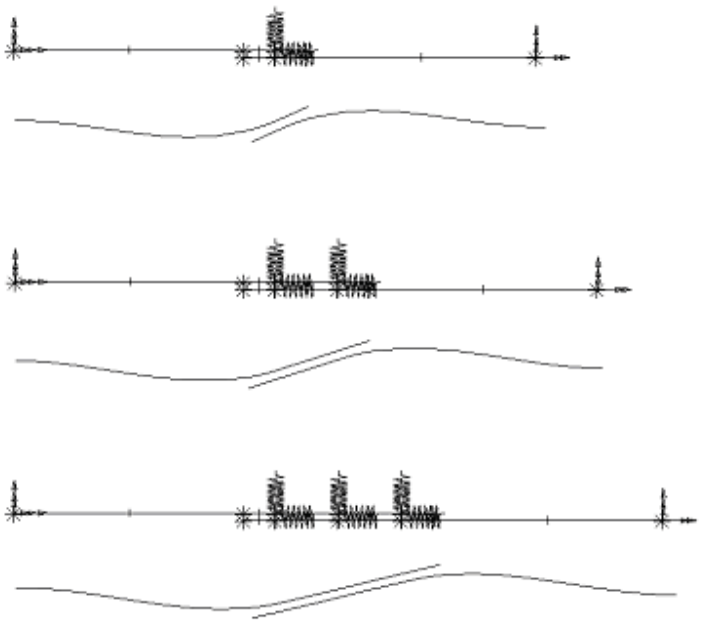

Fig. 8 Model developed thanks to a commercial Finite Element code.

Table 2 Results from the Finite Element model and analytical model

	1 fastener	2 fasteners	3 fasteners
displacement of the end of the joint, mm	0.0104	0.00868	0.008047
load according to the *x* axis taken by the 1st fastener, N	100	50	38.25
load according to the *x* axis taken by the 2nd fastener, N		50	23.5
load according to the *x* axis taken by the 3rd fastener, N			38.25
load according to the *y* axis at the clamped end, N	2.26	1.995	1.767
moment around the *z* axis at the clamped end, N	59.9	57.95	54.6

As a result, the analytical model presented in this paper is able to simulate both boundaries cases (i.e.: the bonded joint and the bolted joint).

D. Results for the Hybrid Single-Lap Joint Configuration

The model provides the normal force, the shear force, and the bending moment in the adherends, and the adhesive shear and peel stresses. The bolt load transfer can be calculated too. From Fig. 9 to Fig. 12 these different functions of the hybrid joint with two fasteners for the parameter values of the previous paragraph are presented.

The influence study of the whole mechanical and geometrical parameters, which is performed thanks to the model, fits the known trends[23] that is to say the load transferred by the fasteners increases when:

- the Young's modulus of adherends increases;
- the thickness of the adherends increases;
- the length of the overlap decreases;
- the Coulomb's modulus of the adhesive decreases;
- the longitudinal pitch between the fasteners decreases.

It is possible to add that the load transferred by the fasteners increases when:

- the stiffness of the fasteners increases;
- the width of adherends decreases;
- the edge distance decreases.

The previous influence study is performed by varying each parameter when the others are set to their nominal values given in Table 1.

The load transfer is rather confined to the extremities of the joint. Hence the edge distance is highly influent relatively to the influence of the longitudinal pitch.

Thanks to the presented model, the influence study is performed easily and quickly. For example, the curve of the influence of the Coulomb's modulus on the bolt load transfer for the balanced hybrid single-lap joint with two fasteners is plotted in Fig. 13. The mechanical and geometrical parameters are defined in Table 1, except the value of the adhesive Coulomb's modulus, which is taken equal to 200 MPa, in order to emphasize the bolt load transfer. The stiffnesses of the fasteners are $C_u = 5.10^4$ N.mm^{-1}, $C_w = 2.10^6$ N.mm^{-1}, $C_\theta = 6.10^6$ N.mm.rad^{-1} and the length of the beams outside the overlap is $l = 70$ mm as in the previous paragraph.

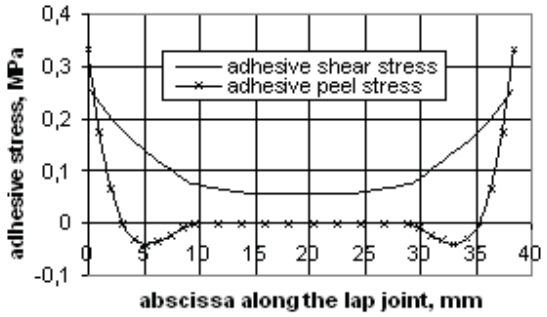

Fig. 9 Adhesive shear stress and adhesive peeling stress along the overlap with f = 100 N.

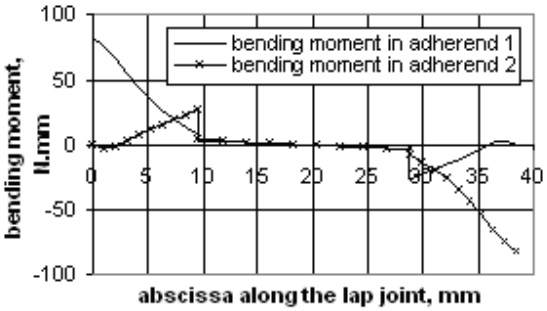

Fig. 10 Bending moment in both adherends along the lap joint with f = 100 N.

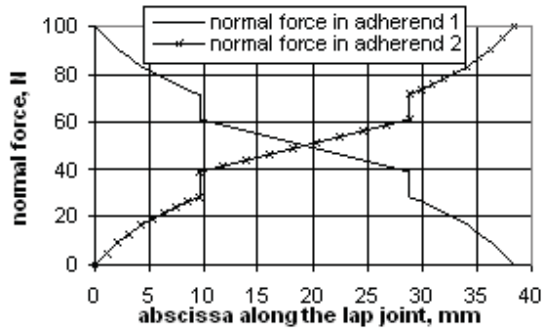

Fig. 11 Normal force in both adherends along the lap joint with f = 100 N.

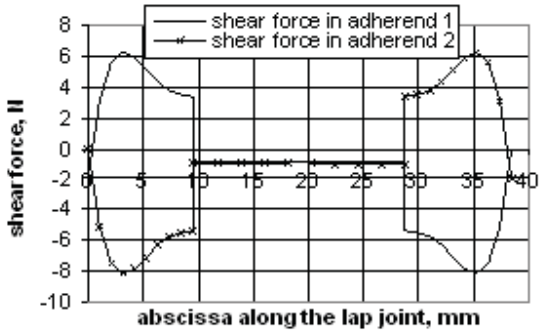

Fig. 12 Shear force in both adherends along the lap joint with f = 100 N.

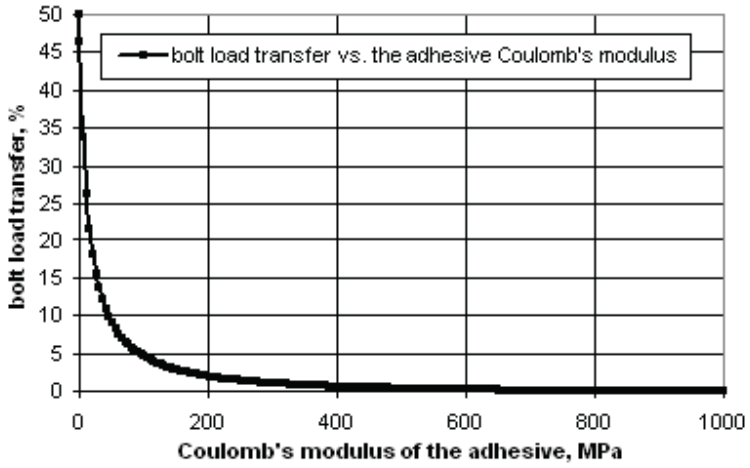

Fig. 13 Bolt load transfer on each bolt as a function of the Coulomb's modulus of the adhesive.

V. Experimental Approach

A campaign of static tests is launched. These tests aim at measuring, on one hand, the bolt load transfer of a two bolts single-lap hybrid joint, and on the other hand, the total displacement of the joint as a function of the applied load, in order to calibrate and validate the results from the analytical model.

A. The Experimental Method

The bolt load transfer is measured with an instrumented bolt.[23] The chosen strain gauges rosettes are manufactured by Tokyosokky under the reference FRA-1-11. The strain gauges are equidistant from the shear plane of the bolt at an angle of 45°. Only one rosette per bolt is used, and, the position of the rosette on the bolts with regard to the joint is marked. An illustration of one instrumented bolt is given in Fig. 14.

In order to deduce the bolt load transferred in the hybrid configuration, a test on a sample, the geometrical and mechanical parameters of which are the same as the hybrid configuration, without bonding but spacing the adherends thanks to filaments the thickness of which is calibrated, is performed. The signals obtained from this reference sample are assumed to represent a load transfer, the rate of which is known as regard the applied load. Then, the signals obtained from the hybrid configuration are compared with this reference, in order to provide the bolt load transfer for the hybrid configuration.

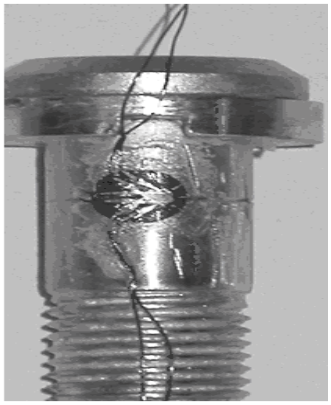

Fig. 14 Instrumented bolt.

The dimensions of the joint are restricted by the dimensions of the strain gauges used for the instrumentation of the bolts. The adherends are manufactured from Aluminum 5086 H111. Both bolts are titanium bolts ASNA 2027, of which the diameter is equal to 9.5 mm. The adherends are drilled with a tolerance of 1.5% with the same numerical command machine for the whole sample according the same fabrication process. A torque of 1 N.m is applied to each bolt. The tests show that this torque is sufficient to prevent the displacement of the calibrated filaments between both adherends and the friction. The adherends are bonded by a two component structural polyurethane adhesive (Pliogrip 7400/7410 by Ashland Speciality Chemical Company). The mechanical characteristics of this adhesive are expected to be able to share the load between the fasteners and the adhesive layer. Its tensile stress-strain behavior can be found in Ref. 23. The geometrical and mechanical parameters of the single-lap configuration used in the experimental approach are given in Table 3.

Table 3 Mechanical and geometrical parameters

E_r, MPa	ν_r	e_r, mm	E_s, MPa	ν_s	e_s, mm	d, mm	s,mm	b, mm	l, mm
69000	0.33	5	620	0.42	0.6	19	38	19	115

The joint is tested under quasi-static tensile load which is performed thanks to a testing machine (Instron 8800) with a 100 kN load cell. The machine is fully computer controlled. The load and the displacement of the grip are recorded by the system. The test is run in load control. Six cycles of linearly load and unload are performed. The first two ones are run until 2 kN and the followings until 14 kN. The level of maximal load is limited in order to stay in the elastic domain and to avoid damage to the instrumented bolts. An illustration of the experimental set-up is given in Fig. 15.

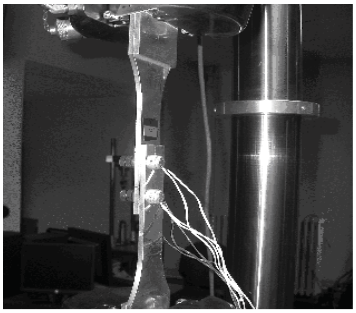

Fig. 15 Experimental set-up.

B. Bolt Load Measurement

The bolt load transfer is measured and deduced according to the method described in the previous paragraph. More precisely, the recorded signals of both instrumented bolts allow to compute the values of the shear strains as a function of the applied load and time for each bolt. According to experimental works[24] using the instrumented bolts the load is not distributed fairly between both lines of bolts: one line of bolts transfers up to 60% of the applied load. The tests campaign allows to show this surprising experimental result. The exploitation of the experimental data is also made from the signal obtained by summing the computed shear strain of both instrumented bolts. As a result, the computed signal obtained for the reference sample is assumed to represent a bolt load transfer of 100%.

From the reference sample, two different ranges of applied load have to be considered. The first range of applied load is located between 0 kN and 3 kN, and the second one is located between 3 kN and 14 kN. In these two ranges of applied load the shear strain is increasing linearly with two different rates. For the case of the hybrid sample, the shear strain can be considered as linearly dependent on the applied load between 0 kN and 14 kN. The linear variation of the shear strain as a function of the applied load shows the bolt load transfer remains constant under low loads, as shown in Fig. 16.

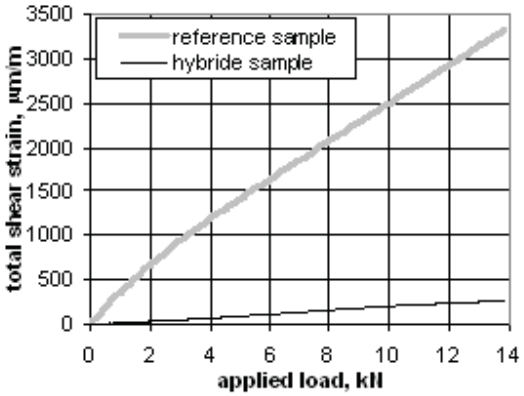

Fig. 16 Total shear strain measured from experimental tests.

For the hybrid case, the range of strain measured corresponds to the range from 0 kN to 3 kN of applied load in the reference case. Consequently, the bolt load transfer is computed by comparing the rates in the range from 0 kN to 3 kN. The total bolt load transfer is 5.6%, and thus 2.8% for each bolt is assumed.

C. Comparison with the Analytical Model

In order to use the analytical model, the stiffnesses of the fasteners have to be estimated. In this paragraph a method is suggested. This method is based on experimental results and on the simulation of the fastener by an elastic beam under shear and bending loads[7].

The stiffness C_w has no influence on the load transfer. By homogeneity with the following stiffnesses, its expression may be computed, like the tensile stiffness of a cylinder, the length of which is the distance between the neutral axes of both adherends, and the diameter is the diameter of the fastener (with $E_f = 110000\ MPa$ and $\phi = 9.5\ mm$):

$$C_w = \frac{E_f \pi \phi^2}{4(e_s + e_r)} \tag{40}$$

From the determination of the fastener longitudinal displacement (along the x axis) due to shear and bending loads,[7] the shear stiffness (C_u) and the bending stiffness (C_θ) are linked by Eq. (41) (with $\nu_f = 0.33$):

$$C_\theta = \frac{3}{8}(1+\nu_f)\phi^2 C_u \tag{41}$$

Consequently, only one stiffness has to be determined. The analytical model provides the total displacement of the joint: it is run with the mechanical and geometrical parameters of the experimental tests, except the mechanical parameters of the adhesive, which are taken very low ($\nu_s = 0.01$ and $E_s.e_s^{-1} = 0.01\ MPa.mm^{-1}$), in order to simulate the test of the reference sample. The value of the shear stiffness, for example, is assumed to be the one, which provides the same total displacement measured during the test of the reference sample. The result value of C_u is 47400 $N.mm^{-1}$. The bolt load transfer associated with this value of the shear stiffness is 2.77% on each fastener according to the analytical model in the hybrid configuration using the values given in Table 3.

However, the behavior of the fasteners in a joint seems to be more complicated, and a three-dimensional model has to be helpful, in order to estimate the shear and bending stiffness fasteners.

VI. Numerical Approach

A parametric three-dimensional model is required in order to understand and to represent accurately the behavior of the hybrid joint. From a parametric three-dimensional model of a bolted single-lap joint[25] developed especially for previous studies about bolted joining using the SAMCEF[26] FE code, a parametric three dimensional of a hybrid single-lap joint is developed.

A. Finite Element Modeling

The FE model is developed using three-dimensional brick elements. More precisely, the adherends and the adhesive are modeled with eight-node elements (24 DoF) and the fasteners are modeled with twenty-node elements (60 DoF). The mesh is particularly refined around the holes and in the adhesive layer (10 elements in the thickness of the adhesive layer).

The symmetry along the length of the lap joint is adopted, so that the study is performed on a half model as shown in Fig. 17. One end of the joint is clamped, whereas the opposite end is free to move in the longitudinal direction only. No pre-tension is applied to the bolt, and no clearance between the adherends and the fasteners is assumed. The contact between the adherends and the fasteners is assumed without friction. A linear behavior of materials, low strains and displacements are assumed. It is sufficient to perform a linear analysis, since the maximal applied load is low enough in order to avoid a too high secondary bending of the joint on one hand, and on the other hand, not to harden the materials.

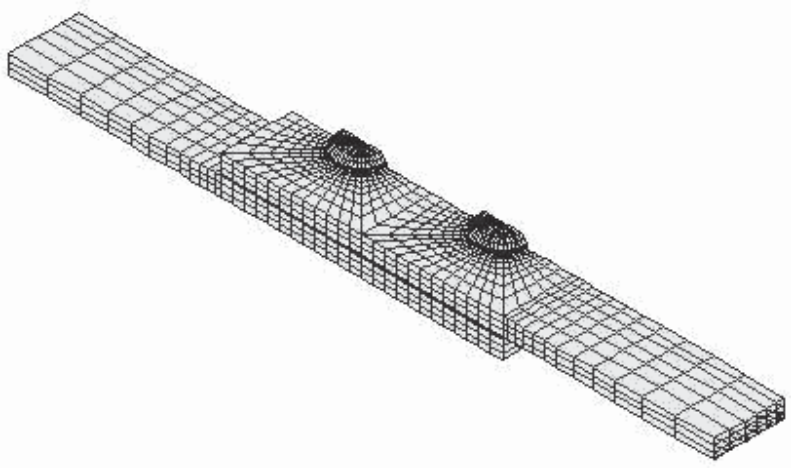

Fig 17 Finite Element model of the hybrid joint in single-lap configuration.

B. Numerical Approach of Shear and Bending Stiffnesses for the Fastener Simulation of the Analytical Model

In order to determine the shear stiffness and the bending stiffness for the fastener simulation of the analytical model, the FE model is used in linear analysis with an adhesive layer, the mechanical properties of which are very low ($\nu_s = 0.01$ and $E_s.e_s^{-1} = 0.01\ MPa.mm^{-1}$), in order to simulate the test of the reference sample. It is noticeable that the tests show a linear behavior under low load. In this case, the sample stiffness given by the FE model is 2.4% below the one measured during the test on the reference sample. The numerical model is thus assumed to represent with good agreement the test performed and can be used to determinate appropriated values of shear and bending stiffnesses.

The shear stiffness is also numerically measured by dividing the load passed by the fastener by the relative displacement between the fasteners and the adherends in its own mid line. The value found for C_u is 45110 N.mm^{-1}. The bending stiffness is numerically measuring by dividing the reaction moment in the fastener by the relative angular displacement between both mid lines of the fasteners and of the adherends. The found value for C_θ is 6156000 N.mm.

The load transfer given by the analytical model, using the value of the Eq. (41) for C_w, is 2.86% on each bolt. Moreover, this approach allows to take into account the local behavior of a fastener through the numerical determination of the local stiffness.

VII. Conclusion

An analytical two-dimensional model of hybrid (bolted/bonded) joint in the balanced single-lap configuration is developed and presented in this paper. An elastic behavior of the materials is assumed. The model is based on the Finite Element Method, so that a special Finite Element (BB element) is computed in order to simulate the bonded adherends. The simulation of a single-lap bonded joint using a BB element shows good agreement with the G&R[10] theory. Moreover, this element provides exact results, and one element per bay is sufficient. The simulation of fasteners is complicated due to the complex behavior of a fastener in a joint, and requires an accurate determination of the local stiffnesses. Two approaches are suggested in order to determine these local stiffnesses. The first approach is based on experimental tests and the beam theory. The second one is based on a numerical three-dimensional FE model, which is validated through experimental tests. Both approaches provide local stiffnesses for the analytical model, which also provides good agreement with the experimental tests, in term of bolt load transfer. The model is fully parametric. As a result, influence studies are launched easily in order to determine the mechanical behavior of the hybrid joint. In order to share the load between the fasteners and the adhesive layer, a flexible adhesive, in particular, has to be used. Consequently, the model presented may be regarded as an efficient, easy to use and fast design tool, when it is accurately calibrated.

Three ways are under consideration to continue. The first way is the development of the imbalanced BB element. Moreover, the integration of a perfectly elastic-plastic and of a viscoelastic adhesive behavior in the BB element is imaginable. The simulation of the fasteners has to be studied too. The second way is the launch of fatigue tests, in order to validate the reliability of the hybrid joints. The third way is the exploitation of the numerical model, in order to understand accurately the mechanical behavior of hybrid joining.

Appendix

The stiffness matrix of the beams outside the lap is:

$$K_{beam} = E_r \begin{pmatrix} S_r l^{-1} & -S_r l^{-1} & 0 & 0 & 0 & 0 \\ -S_r l^{-1} & S_r l^{-1} & 0 & 0 & 0 & 0 \\ 0 & 0 & 12 I_r l^{-3} & -12 I_r l^{-3} & 6 I_r l^{-2} & 6 I_r l^{-2} \\ 0 & 0 & -12 I_{r1} l^{-3} & 12 I_r l^{-3} & -6 I_r l^{-2} & -6 I_r l^{-2} \\ 0 & 0 & 6 I_r l^{-2} & -6 I_r l^{-2} & 4 I_r l^{-1} & 2 I_r l^{-1} \\ 0 & 0 & 6 I_r l^{-2} & -6 I_r l^{-2} & 2 I_r l^{-1} & 4 I_r l^{-1} \end{pmatrix} \quad (42)$$

The integration constants are given by the Eq. (41) to Eq. (52):

$$c_1 = \frac{(u_l + u_k) - (u_i + u_j)}{\Delta} \tag{43}$$

$$c_2 = u_i + u_j \tag{44}$$

$$c_3 = w_j - w_i \tag{45}$$

$$\begin{aligned} &c_6\left(\frac{\sinh(\sigma\Delta)}{\sin(\sigma\Delta)} - \frac{\sin(\sigma\Delta)}{\sinh(\sigma\Delta)}\right) = \\ &-(w_j - w_i)\left(\frac{\cos(\sigma\Delta)}{\sinh(\sigma\Delta)} + \frac{\cosh(\sigma\Delta)}{\sin(\sigma\Delta)}\right) + (w_l - w_k)\left(\frac{\cosh(\sigma\Delta)}{\sinh(\sigma\Delta)} + \frac{\cos(\sigma\Delta)}{\sin(\sigma\Delta)}\right) - \frac{(\theta_l - \theta_k)}{\sigma} - \frac{(\theta_j - \theta_i)}{\sigma}\frac{\sin(\sigma\Delta)}{\sinh(\sigma\Delta)} \end{aligned} \tag{46}$$

$$c_5 = \frac{(\theta_j - \theta_i)}{\sigma} - c_6 \tag{47}$$

$$c_4 shs(\sigma\Delta) = (w_l - w_k) - chc(\sigma\Delta)(w_j - w_i) - chs(\sigma\Delta)\frac{(\theta_j - \theta_i)}{\sigma} - (shc(\sigma\Delta) - chs(\sigma\Delta))c_6 \tag{48}$$

$$\begin{aligned} &c_{11}\left(\frac{-\Delta^3}{3e_r} + \frac{8\mu^2}{e_r\eta^2\rho^3}\frac{ch-1}{sh} - 4\frac{\Delta}{e_r}\frac{\mu^2}{\eta^2\rho^2}\right) = (w_l + w_k) - \\ &(w_i + w_j) - \left(\frac{\Delta}{e_r} + \frac{2}{e_r\rho}\frac{1-\cosh(\rho\Delta)}{\sinh(\rho\Delta)}\right)\frac{\mu^2}{\rho^2}\left[(u_l - u_k) + (u_j - u_i)\right] - \left(\frac{\Delta\eta^2}{2} - \frac{\mu^2}{\rho}\frac{1-\cosh(\rho\Delta)}{\sinh(\rho\Delta)}\right)\frac{1}{\rho^2}\left[(\theta_l + \theta_k) + (\theta_i + \theta_j)\right] \end{aligned} \tag{49}$$

$$c_8 = \frac{\eta^2}{\rho^2}\frac{\left[(u_l - u_k) - \frac{e_r}{2}(\theta_l + \theta_k)\right] - e^{-\rho\Delta}\left[(u_j - u_i) - \frac{e_r}{2}(\theta_i + \theta_j)\right]}{2\sinh(\rho\Delta)} - 2c_{11}\rho^{-2}\frac{1 - e^{-\rho\Delta}}{2\sinh(\rho\Delta)} \tag{50}$$

$$c_7 = \frac{\eta^2}{\rho^2}\frac{-\left[(u_l - u_k) - \frac{e_r}{2}(\theta_l + \theta_k)\right] + e^{\rho\Delta}\left[(u_j - u_i) - \frac{e_r}{2}(\theta_i + \theta_j)\right]}{2\sinh(\rho\Delta)} + 2c_{11}\rho^{-2}\frac{1 - e^{\rho\Delta}}{2\sinh(\rho\Delta)} \tag{51}$$

$$c_9 = \frac{\mu^2}{\rho^2}(u_j - u_i) + \frac{\eta^2}{\rho^2}\frac{e_r}{2}(\theta_i + \theta_j) + 2c_{11}\rho^{-2} \tag{52}$$

$$c_{10}\Delta = \frac{\mu^2}{\rho^2}\left[\left(u_l - u_k\right) - \left(u_j - u_i\right)\right] + \frac{\eta^2}{\rho^2}\frac{e_r}{2}\left[\left(\theta_l + \theta_k\right) - \left(\theta_i + \theta_j\right)\right] - \Delta^2 c_{11} \tag{53}$$

$$c_{12} = \left(w_i + w_j\right) + \frac{2}{e_r}\frac{\mu^2}{\eta^2}\frac{1}{\rho}\left(c_8 - c_7\right) \tag{54}$$

Acknowledgments

This study is performed in cooperation with AIRBUS (Toulouse and Saint-Nazaire, France). The authors are grateful to the industrial partners for their advice and support.

References

[1]Tate, M. B., and Rosenfeld, S. J., "Analytical and Experimental Investigation of Bolted Joint," NACA TN-1458, 1947.

[2]Ross, R. D., "An Electrical Computer for the Solution of Shear-Lag Bolted Joint Problem," NACA TN-1281, 1947.

[3]Huet, J., "Du calcul des assemblages par boulons ou rivets travaillant en cisaillement," AEROSPATIALE Aéronautique CO/Airbus, Toulouse, France (unpublished).

[4]Unpublished Reports of the BOEING Corporation, Renton WA.

[5]Swift, T., "Development of the Fail-Safe Design Features of the DC-10," *Damage Tolerance in Aircraft Structures*, *ASTM STP 486*, *American Society for Testing and Materials*, Philadelphia, 1970, pp. 164-214.

[6]Huth, H., "Influence of Fastener Flexibility on the Prediction of Load Transfer and Fatigue Life for Multiple-Row Joints," *Fatigue in Mechanically Fastened Composite and Metallic Joints, ASTM STP 927*, *American Society for Testing and Materials*, Philadelphia, 1986, pp. 221-250.

[7]Cope, D. A., and Lacy, T.E., "Stress Intensity Determination in Lap Joints with Mechanical Fasteners," *Presented at 41st AIAA Structures, Structural Dynamics, and Materials Conference and Exhibit*, AIAA 2000-1368, 3-6 April 2000, Atlanta GA.

[8]Cramer, C. O., "Load Distribution in Multiple Bolt Tension Joints," *Journal of the structural Division*, Vol. 94, No. 5, 1968, pp. 1101-1117.

[9]Volkersen, O., "Die Nietkraftverteilung in Zugbeanspruchten Nietverbindungen mit Konstanten Laschenquerschnitten," *Luftfahrtforschung*, Vol. 15, 1938, pp. 41-47.

[10]Goland, M., and Reissner, E., "The Stress in Cemented Joints," *Journal of Applied Mechanics*, Vol. 11, No. 1, 1944, pp. A-17-27.

[11]Hart-Smith, L. J., "Adhesive-Bonded Double-Lap Joints," NASA CR-112235, 1973.

[12]Hart-Smith, L. J., "Adhesive-Bonded Single-Lap Joints," NASA CR-112236, 1973.

[13]Allman, D. J., "A Theory for Elastic Stresses in Adhesive Bonded Lap Joints," *International Journal of Mechanics and Applied Mathematics*, Vol. 30, 1977, pp. 415-436.

[14]Renton, W. J., and Vinson, J. R., "Analysis of Adhesively Bonded Joints Between Panels of Composite Materials," *Journal of Applied Mechanics*, 1977, pp. 101-106.

[15]Erdogan, F., and Ratwani, M., "Stress Distribution in Bonded Joint," *Journal of Composite Materials*, Vol. 5, 1971, pp. 378-393.

[16]Carpenter, W.C., and Barsoum R., "Two Finite Elements for Modeling the Adhesive in Bonded Configurations," *Journal of Adhesion*, Vol. 30, pp. 25-46.

[17]Amijima S., and, Fuji T., "A Microcomputer Program for Stress Analysis of Adhesive-Bonded Joints," *International Journal of Adhesion and Adhesives*, Vol. 7, No. 4, 1987, pp. 199-204.

[18]Adams, R. D., and Mallick, V., "A method for the Stress Analysis of Aluminium-Aluminium Bonded Joints," *Journal of Adhesion*, Vol. 38, 1992, pp. 199-217.

[19]Paroissien, E., Sartor, M., and Huet J., "Hybrid (bolted/bonded) Joints Applied to Aeronautic Parts: Analytical One-Dimensional Models of a Single-Lap Joint," *6th International Conference of Integrated Design and Manufacturing in Mechanical Engineering*, 17-19 May 2006, Grenoble, France.

[20]Turner, M. J., Martin, H. C., Weikel, R. C., "Further development and applications of the stiffness method, in AGARDograph 72: Matrix Methods of Structural Analysis", ed. by B. M. Fraeijs deVeubeke, Pergamon Press, New York, 1964, pp. 203-266.

[21]MATLAB, Service Pack 1, Ver. 6.5.1. Release 13, August 2003, The MathWorks, inc.

[22]I-DEAS, Ver. 11, UGS Group.

[23]Kelly, G., "Joining of Carbon Fibre Reinforced Plastics for Reinforced Applications," Ph. D. Dissertation, Department of Aeronautical and Vehicle Engineering, Royal Institute of Technology, Stockholm, Sweden, 2004.

[24]Starikov, R., "Mechanically fastened joints: Critical testing of single overlap joint," FOI Swedish Defence Research Agency, Scientific Report, FOI-R—0441—SE, ISSN 1650-1942, March 2002.

[25]Esquillor, J., Huet, J., and Lachaud, F., "Modélisation par éléments finis d'un assemblage aéronautique en simple cisaillement," *Presented at 17th Congrès Français de Mécanique*, *Paper on Disc* [Paper No. 354], September 2005, Troyes, France.

[26]SAMCEF, Ver. 11.1-01., Samtech Group.